

# An asynchronous BMI for autonomous robotic grasping based on SSVEF detection

C. Reichert<sup>1,2,3</sup>, M. Kennel<sup>4</sup>, R. Kruse<sup>2</sup> and H. Hinrichs<sup>1,3</sup>

<sup>1</sup> Dept. of Neurology, University Medical Center A.ö.R., Magdeburg, Germany  
christoph.reichert@med.ovgu.de, hermann.hinrichs@med.ovgu.de

<sup>2</sup> Dept. of Knowledge and Language Processing, Otto-von-Guericke University, Magdeburg, Germany

<sup>3</sup> Forschungscampus STIMULATE, Magdeburg, Germany

<sup>4</sup> Fraunhofer Institute for Factory Operation and Automation IFF, Magdeburg, Germany

## Abstract

Severely impaired persons could greatly benefit from assistive devices controlled by brain activity. However, the low information transfer rate of noninvasive neuroimaging techniques complicates complex and asynchronous control of robotic devices enormously. In this paper we present an asynchronous brain-machine interface (BMI) relying on autonomous grasp planning. The system enables a user to grasp and manipulate objects with a minimal set of commands. We successfully tested the system in a virtual environment with eight subjects. Our results suggest that the system represents a promising approach for real-world application of brain-controlled intelligent robotic devices.

## 1 Introduction

One of the most convenient applications of brain-machine interfaces is the control of prosthetic devices. Many approaches have been developed so far, including non-invasive [1] and invasive [2] control of an artificial upper limb. However, for continuous control, the commonly performed decoding of motor sensory rhythms, originated in motor imagery, has two drawbacks: due to only a few distinguishable classes the degrees of freedom to control the effector are limited and the training phase for users is long. An alternative control signal is the steady state visual evoked potential (SSVEP) which provides a robust signal for detection and an easy usage. In a previous study [3] we showed that the magnetic fields induced by SSVEPs (steady state visual evoked field, SSVEF) can be reliably decoded to select virtual reality objects. The control of a robotic hand with SSVEP detection was presented by [4] but still the degrees of freedom which can be controlled are very limited. Here we present an SSVEF based prototype system, aimed at autonomously grasping and manipulating objects, which is controlled asynchronously via visual overt attention. The decoding scheme we applied is designed to minimize erroneous actions of the manipulator which facilitates successful and secure grasping when combined with an intelligent actuator.

## 2 Methods

### 2.1 Robotic Grasping System

We developed a virtual reality scenario designed to simulate the control of a robotic device. Virtual objects, placed in the working area of the robot, can be grasped autonomously by the robot [5, 6]. In the current setup we placed four spherical objects on the table serving as potential grasp targets. Furthermore, we placed a green start button and a red stop button on the table to send control commands to the robot. All objects were tagged with stimulation

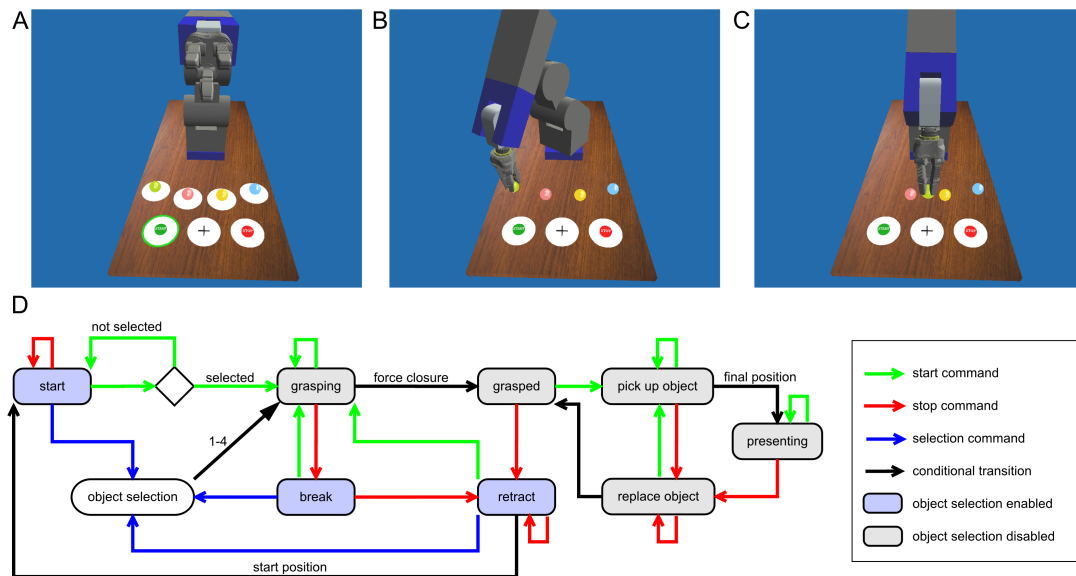


Figure 1: Robotic gripper in the states *start* (A), *grasped* (B) and *presenting* (C) and the state diagram (D) of the system which is controllable by only three commands (start, stop and object#).

surfaces flickering at different frequencies (object 1–4: 6.818 Hz, 7.5 Hz, 8.333 Hz, 9.375 Hz; start button: 10.714 Hz; stop button: 12.5 Hz). Whenever only the selection of a command button was reasonable, e.g. during a running grasping process, the stimulation of objects 1–4 was stopped. Thus, selection of a new object to grasp was only possible when the gripper was in the states *retract*, *break* and *start*. This reduces the probability of unwanted selections during the grasping and manipulation process. As a representative manipulation the object could be picked up and presented. For resting periods, a non-flickering area, e.g. the fixation cross must have been focused. For the selection of the object to be grasped next, the corresponding flickering surface has to be attended. The selection of the start button initiates a grasp to the lastly selected object, the presentation of the object and the resuming of a stopped grasp movement. In contrast, a selection of the stop button causes the reverse operations. Figure 1 (D) visualizes the state transitions of the robot dependent on activation of the start button (green transitions) and the stop button (red transitions). States marked in grey indicate stimulation of start and stop button only, states marked in blue indicate stimulation of all six surfaces.

## 2.2 Decoding Algorithm

We decoded the SSVEF by means of canonical correlation analysis (CCA) [7]. This method finds the optimal weighting  $W_{x,f}$  and  $W_{y,f}$  of input channels  $X$  (here the signals of 59 occipital MEG sensors) and model channels  $Y_f$  (sine and cosine waves of the stimulation frequency  $f$  and optionally harmonics) to maximize the correlation  $\rho_{CCA}(f)$  between linear combinations  $x_f = X^T W_{x,f}$  and  $y_f = Y_f^T W_{y,f}$ . The CCA was applied to MEG data asynchronously every 1000 ms from the preceding 2000 ms interval. To distinguish resting intervals from selection intervals, we determined a confidence threshold  $th_f$  for each frequency  $f$  from the empirical

distribution of coefficients  $\rho_{CCA}$  which we revealed in calibration runs. Finally, the classification was determined according to the frequency  $f_{max} = \operatorname{argmax}(\rho_{CCA}(f))$  that revealed the maximum correlation coefficient and exceeded the threshold  $th_f$ .

Feedback of the instantaneous target detection of the decoder was presented at each decoding step by coloured rings around the decoded target. Only after three successive predictions of the same target it was finally selected. The stage of prediction was indicated by stepwise colour changes from light blue to green for the final selection. After a selection, the next decoding was performed three seconds after feedback presentation. The detection of a resting period was displayed at the fixation cross identical to the selectable targets and did not affect the prediction stage of targets.

### 2.3 Experimental Setup

Eight healthy subjects (age 21–34 years) participated in this study. MEG data were acquired with a 248 magnetometer 4DNeuroimaging system, at a sampling rate of 678.17 Hz.

The task of the subjects was to control the autonomously grasping robot depicted in Figure 1 (A–C) by overtly attending the flickering surfaces. The experiment started with calibration runs in which one of six targets or the fixation cross was cued by a black ring during each trial. If the final selection was different from the cued target a red ring indicated the erroneous decoding. A trial was counted as false after 30s of selection failure. The subjects performed 3–4 calibration runs to obtain a reliable performance estimate of the proposed decoding scheme. Additional 3–4 runs were performed to control the robot. In these runs, a high amount of resting periods was required due to the slow movement of the robot. Consequently, relatively few selection trials were performed. Subjects were instructed to grasp, pick up and replace the objects in a predefined order, which was announced by the experimenter directly before the run. In case of an unwanted selection due to erroneous SSVEF detection, the subject had to perform the consequential selection to continue the desired workflow. The sequence of control commands was as follows: Select the object to be grasped, select the start button to grasp the object, select the start button to present the object, select the stop button to replace the object, select the stop button to retract the gripper. In intervals of robot movement, subjects had to prevent selections.

## 3 Results

Although feedback was provided from the first run the decoding of resting intervals started with the second run, when initial calibration data were available. On average, 74% of target trials ( $T_{corr}/trials$ ) and 73% of resting trials ( $R_{corr}/trials$ ) were decoded correctly while the guessing level was 14%. Average selection time  $t_{select}$  was 11.7s while fastest possible selection was 5s. In robot control runs, the speed of a complete grasp sequence ( $G_{compl}/time$ ) was  $0.52 \text{ min}^{-1}$  on average. In order to safely perform gripper control, the movement of the robot was relatively slow (grasping: 28s, picking up: 8s) such that an optimal complete grasp sequence, without complete retracting but including selections, was possible in at least 69s (maximum  $G_{compl}/time = 0.87 \text{ min}^{-1}$ ). As an important result, in our setup false object selections ( $S_{err}$ ) occurred reasonably (26%) but accidentally initiated robot commands ( $C_{err}$ ) occurred rarely (4.7%) although long intervals of preventing erroneous selections were required. Table 1 summarizes the results. The number of trials performed depends on the latency of a final selection and on the number of unwanted selections. One of the subjects was able to perfectly control the system without any erroneous selection.

| Subject<br># | Calibration           |                       |                     | Robot control        |                      |                      |
|--------------|-----------------------|-----------------------|---------------------|----------------------|----------------------|----------------------|
|              | $T_{corr}$<br>/trials | $R_{corr}$<br>/trials | $t_{select}$<br>[s] | $G_{compl}$<br>/time | $C_{err}$<br>/trials | $S_{err}$<br>/trials |
| 1            | 56 / 75               | 18 / 25               | 12.1                | 8.2 / 18'04"         | 3 / 38               | 3 / 14               |
| 2            | 11 / 27               | 4 / 10                | 16.5                | 7.4 / 24'04"         | 8 / 44               | 2 / 13               |
| 3            | 62 / 62               | 23 / 23               | 10.9                | 16.6 / 24'06"        | 0 / 67               | 0 / 20               |
| 4            | 40 / 63               | 15 / 23               | 10.7                | 10.2 / 24'23"        | 2 / 44               | 6 / 26               |
| 5            | 46 / 64               | 21 / 23               | 10.5                | 12.4 / 24'22"        | 1 / 50               | 13 / 33              |
| 6            | 46 / 54               | 17 / 21               | 12.8                | 12.6 / 24'48"        | 1 / 60               | 4 / 24               |
| 7            | 60 / 69               | 16 / 25               | 9.7                 | 15.0 / 21'39"        | 1 / 61               | 14 / 35              |
| 8            | 45 / 67               | 16 / 23               | 10.3                | 10.3 / 23'39"        | 1 / 53               | 21 / 38              |

Table 1: Subject performance

## 4 Conclusions

As an alternative modality to EEG we probed the MEG for detecting SSVEFs. Provided that the EEG allows for comparable detection success, our results indicate that an intelligent actuator in combination with noninvasive detection of SSVEPs could help severely paralyzed patients to initiate complex grasp movements asynchronously. The presented system allows for voluntary robot control with a low error rate even in subjects with moderate selection performance, indicating that noninvasive BMIs may be suitable for grasping despite its low information transfer rate. It is important to note that the transfer of the system into an EEG-driven real-world setting requires further development towards more elaborated stimulus presentation techniques and intelligent prostheses. In addition, a combination with other modalities, for instance tracking of eye movements, could serve to make the system even more robust.

## References

- [1] G. R. Müller-Putz, R. Scherer, G. Pfurtscheller, and R. Rupp. EEG-based neuroprosthesis control: a step towards clinical practice. *Neuroscience Letters*, 382(1-2):169–174, 2005.
- [2] L. R. Hochberg, D. Bacher, B. Jarosiewicz, N. Y. Masse, J. D. Simeral, J. Vogel, S. Haddadin, J. Liu, S. S. Cash, P. van der Smagt, and J. P. Donoghue. Reach and grasp by people with tetraplegia using a neurally controlled robotic arm. *Nature*, 485(7398):372–375, 2012.
- [3] C. Reichert, M. Kennel, R. Kruse, H. Hinrichs, and J. W. Rieger. Efficiency of SSVEF recognition from the magnetoencephalogram - A comparison of spectral feature classification and CCA-based prediction. In *Proceedings of the International Congress on Neurotechnology, Electronics and Informatics*, pages 233–237. SciTePress Digital Library, Sep 2013.
- [4] G. R. Müller-Putz and G. Pfurtscheller. Control of an electrical prosthesis with an SSVEP-based BCI. *IEEE Trans Biomed Eng*, 55(1):361–364, 2008.
- [5] C. Reichert, M. Kennel, R. Kruse, H.-J. Heinze, U. Schmucker, H. Hinrichs, and J. W. Rieger. Robotic grasp initiation by gaze independent brain-controlled selection of virtual reality objects. In *Proceedings of the International Congress on Neurotechnology, Electronics and Informatics*, pages 5–12. SciTePress Digital Library, Sep 2013.
- [6] M. Kennel, C. Reichert, U. Schmucker, H. Hinrichs, and J. W. Rieger. A robot for brain-controlled grasping. In *Proceedings of the Human-Robot Interaction Workshop*, March 2014.
- [7] Z. Lin, C. Zhang, W. Wu, and X. Gao. Frequency recognition based on canonical correlation analysis for SSVEP-based BCIs. *IEEE Trans Biomed Eng*, 54(12):1172–1176, 2007.